Supplementary Information

Stabilizing Surface of Ni-Rich Cathode via Facing-Target Sputtering for High-Performance Lithium-Ion Batteries

Jong Heon Kim[a,b,1], Jun-Seob Park[a,1], Su-Ho Cho[b,1], Ji-Min Park[a], Jong Seok Nam[c], Soon-Gil Yoon[a], Il-Doo Kim[c,], Ji-Won Jung[d,]* and Hyun-Suk Kim[a,]**

[a] Department of Materials Science and Engineering, Chungnam National University, Daejeon 34134, Republic of Korea

[b] Texas Materials Institute and Materials Science and Engineering Program, The University of Texas at Austin, TX 78712, Austin, USA

[c] Department of Materials Science and Engineering, Korea Advanced Institute of Science and Technology (KAIST), 291 Daehak-ro, Yuseong-Gu, Daejeon, 34141, Republic of Korea

[d] School of Materials Science and Engineering, University of Ulsan, Techno saneop-ro 55 beon-gil, Nam-gu, Ulsan 44776, Republic of Korea

Corresponding Author*: Prof. Hyun-Suk Kim, Prof. Ji-Won Jung, Prof. Il-Doo Kim

Email Address: khs3297@cnu.ac.kr, jwjung4@ulsan.ac.kr & idkim@kaist.ac.kr

Figure Captions

Fig. S1. EDS mapping for elements of (a) A(3)-NCM and (b) F(3)-NCM for Ni (sky blue), Co (Green), and Mn (Purple).

Fig. S2. XPS data of P-NCM, A(3)-NCM, and F(3)-NCM for the (a-c) Li 1s and (d-f) O 1s core-level spectra.

Fig. S3. XPS analysis of P-NCM, A(3)-NCM, and F(3)-NCM for the (a) Ni 2p, (b) Co 2p and (c) Mn 2p.

Fig. S4. Nyquist plots of P-NCM, A-NCM and F-NCM, presented with fitted curves.

Fig. S5 (a) Rate capability, (b) Electrochemical impedance spectroscopy data, and (c) Cycling performance of A(1)-NCM, and A(5)-NCM.

Fig. S6 (a) Rate capability, (b) Electrochemical impedance spectroscopy data, and (c) Cycling performance of F(1)-NCM, and F(5)-NCM.

Fig. S7. XPS data of P-NCM, A(3)-NCM, and F(3)-NCM for the (a-c) Li 1s and (d-f) O 1s core-level spectra after 100 cycles.

Fig. S8. XPS anlaysis of P-NCM, A(3)-NCM, and F(3)-NCM for the (a) Ni 2p, (b) Co 2p and (c) Mn 2p after 100 cycles.

Fig. S9. TEM images of (a) A(3)-NCM and (b) F(3)-NCM, EDS mapping for elements of A(3)-NCM and F(3)-NCM for Al (Red), Ni (Sky blue), Co (Green), and Mn (Purple).

Fig. S10. ToF-SIMS profiles of (A) P-NCM, (B) A(3)-NCM, and (C) F(3)-NCM after 100 cycles.

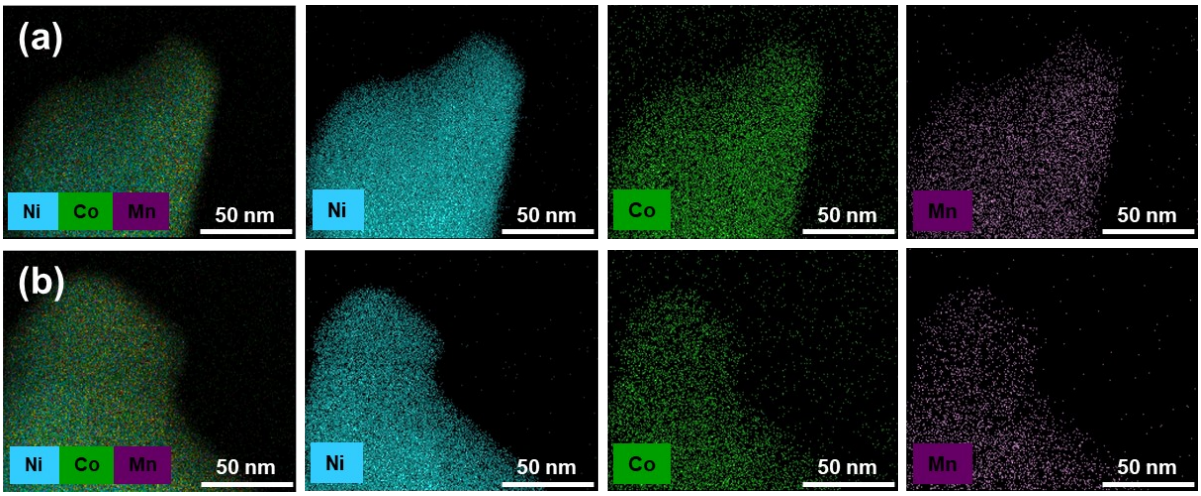

Fig. S1 EDS mapping for elements of (a) A(3)-NCM and (b) F(3)-NCM for Ni (Sky blue), Co (Green), and Mn (Purple).

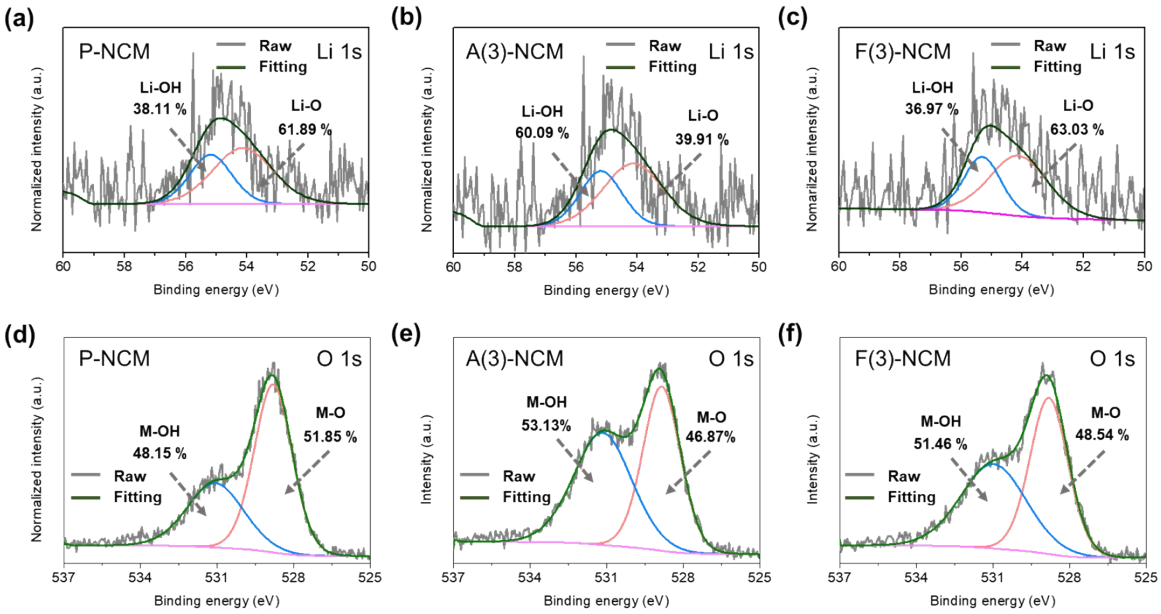

Fig. S2 XPS data of P-NCM, A(3)-NCM, and F(3)-NCM for the (a-c) Li 1s and (d-f) O 1s core-level spectra.

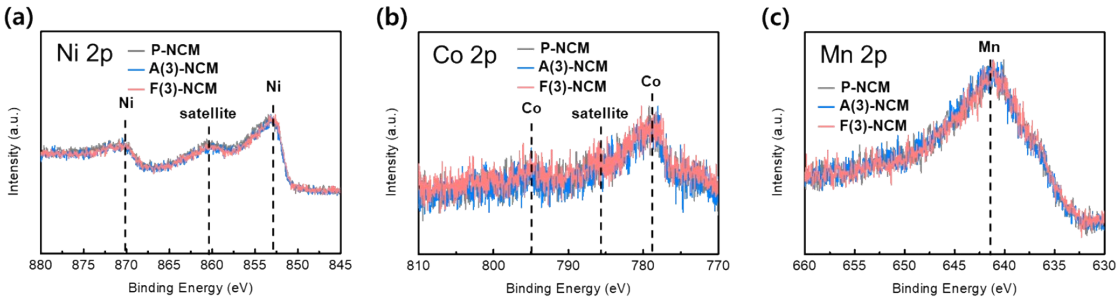

Fig. S3 XPS analysis of P-NCM, A(3)-NCM, and F(3)-NCM for the (a) Ni 2p, (b) Co 2p and (c) Mn 2p.

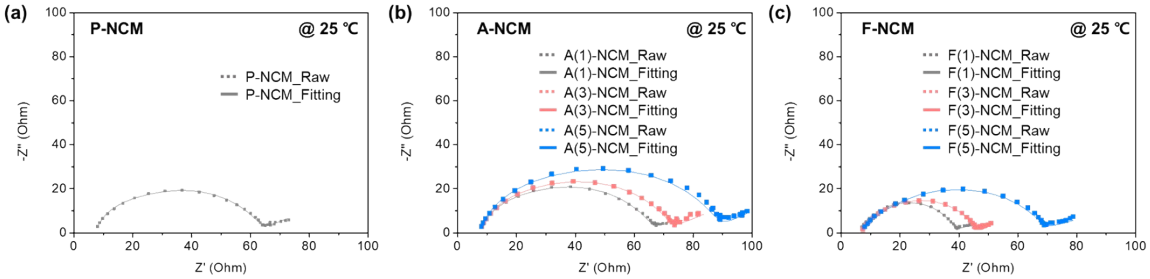

Fig. S4 Nyquist plots of P-NCM, A-NCM and F-NCM, presented with fitted curves.

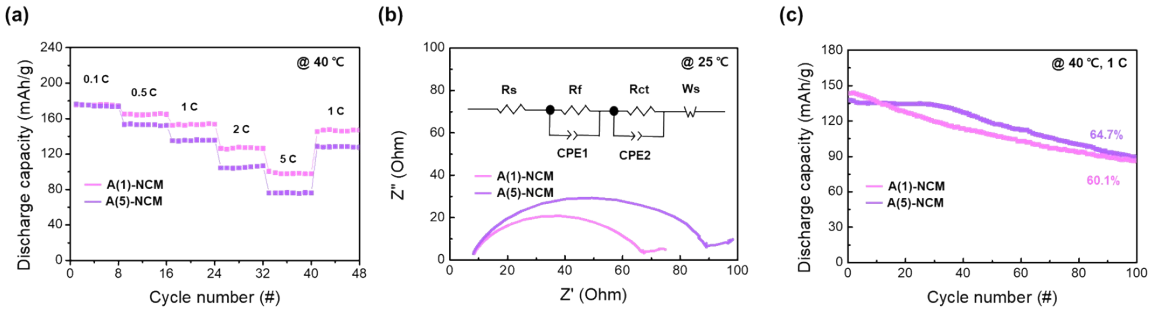

Fig. S5 (a) Rate capability, (b) Electrochemical impedance spectroscopy data, and (c) Cycling performance of A(1)-NCM, and A(5)-NCM.

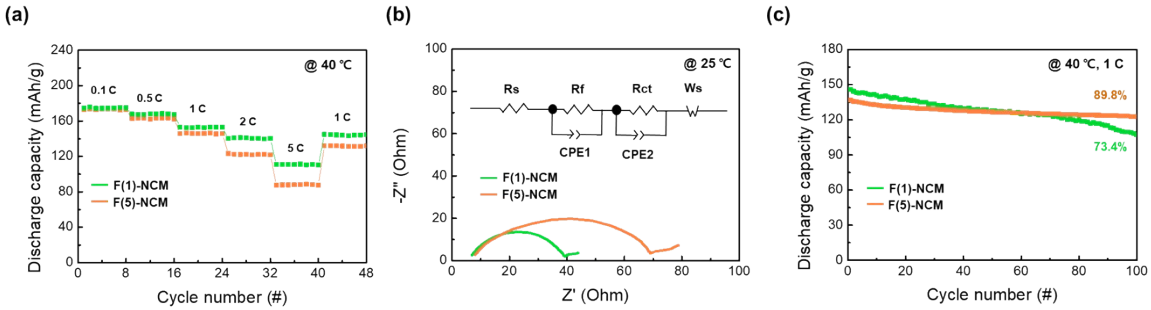

Fig. S6 (a) Rate capability, (b) Electrochemical impedance spectroscopy data, and (c) Cycling performance of F(1)-NCM, and F(5)-NCM.

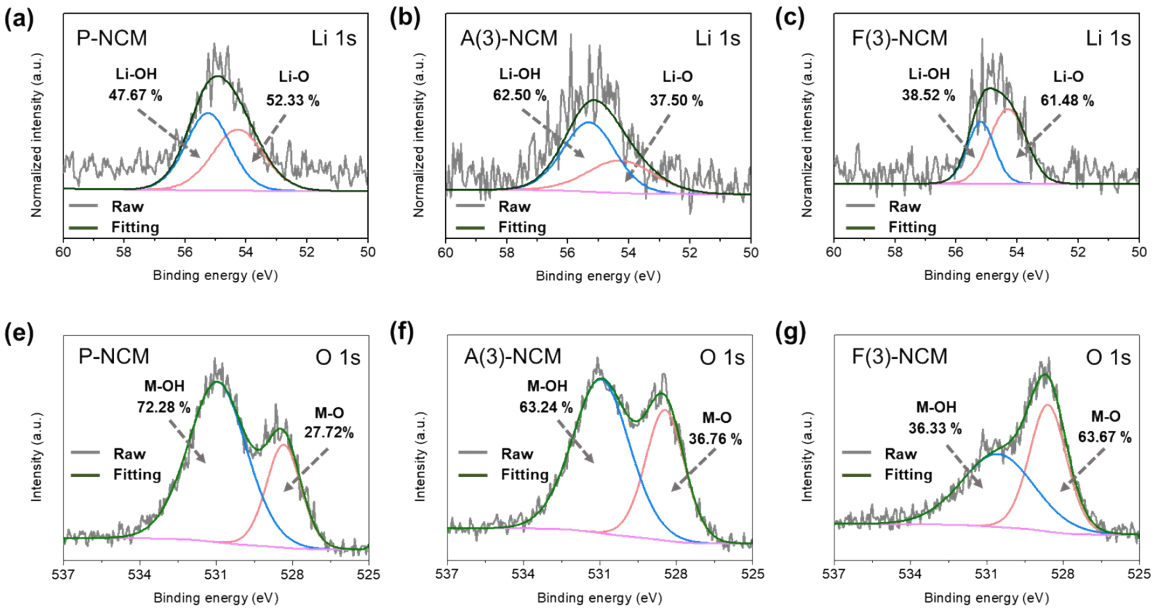

Fig. S7 XPS data of P-NCM, A(3)-NCM, and F(3)-NCM for the (a-c) Li 1s and (d-f) O 1s core-level spectra after 100 cycles.

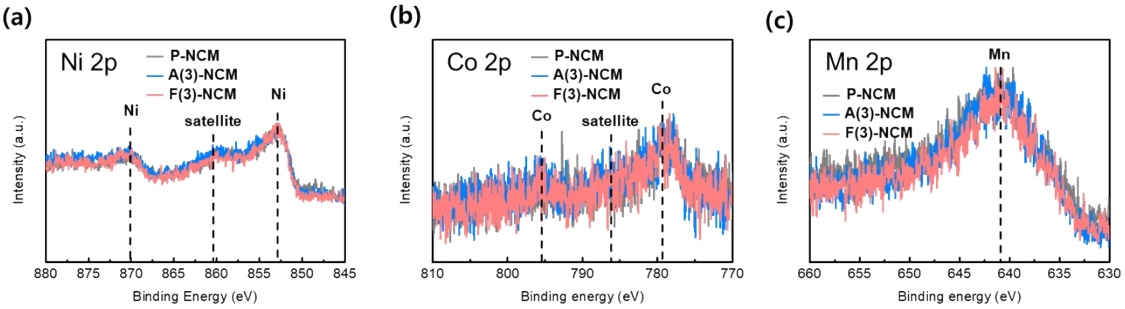

Fig. S8 XPS analysis of P-NCM, A(3)-NCM, and F(3)-NCM for the (a) Ni 2p, (b) Co 2p and (c) Mn 2p after 100 cycles.

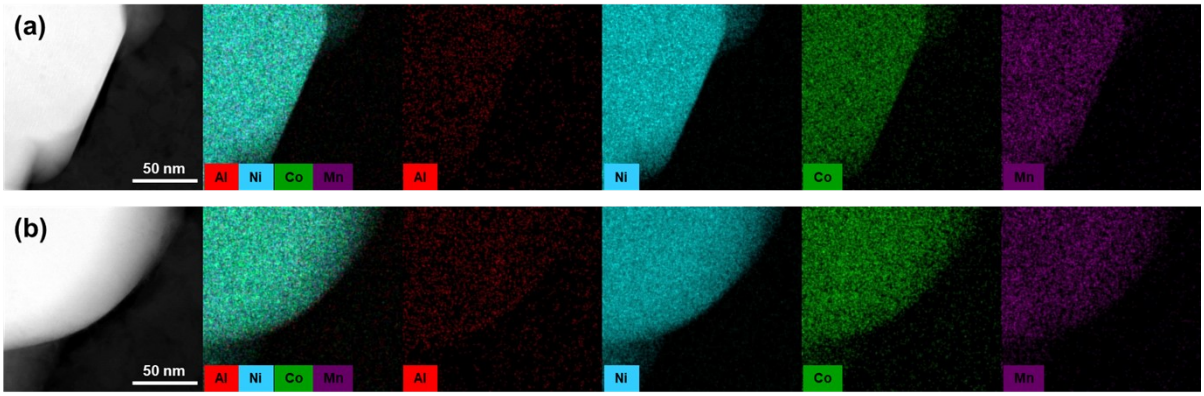

Fig. S9 TEM images of (a) A(3)-NCM and (b) F(3)-NCM, EDS mapping for elements of A(3)-NCM and F(3)-NCM for Al (Red), Ni (Sky blue), Co (Green), and Mn (Purple).

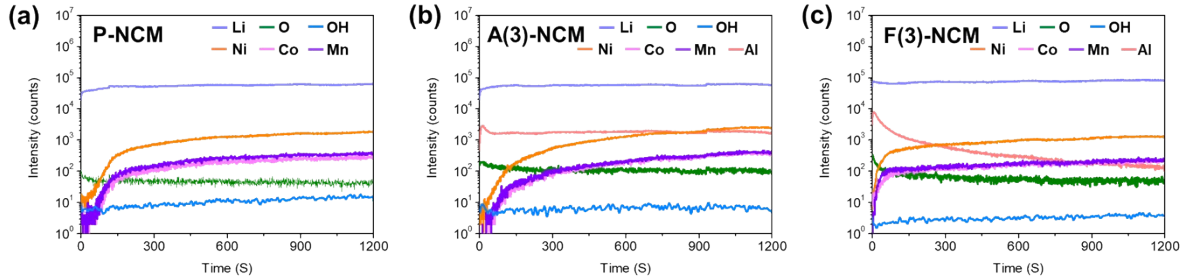

Fig. S10 ToF-SIMS profiles of (A) P-NCM, (B) A(3)-NCM, and (C) F(3)-NCM after 100 cycles.